

# Linear Tape Recording Channels

Volker Braun,

Institute for Experimental Mathematics, Ellernstr. 29, 45326 Essen, Germany,

Phone: +49 201 3206448, Fax: +49 201 3206463, E-mail: volker@exp-math.uni-essen.de.

**Abstract**—We will apply Golay complementary sequences for measuring the impulse response and the amplitude and phase transfer functions of a linear magnetic tape recording channel. Our experimental channel suffers from nonlinear distortion caused by a magnetoresistive sensor. The measured characteristics, in particular the amplitude transfer function, show better performance than the same characteristics obtained with the de facto standard impulse response measurement technique using feedback shift register sequences. Based on a practical nonlinear Volterra model of our experimental tape recording channel, we will analyze the artefacts due to second and third order nonlinear distortion which can occur in the Golay impulse responses and transfer functions.

## I. INTRODUCTION

A digital signal processing technique based on Golay complementary sequences [2] has attracted considerable attention for measuring the impulse responses of linear time-invariant systems. A detailed description of this Golay technique can be found in, for example, [1]. Applications of this technique have been described in, for example, [1], [5], or [12]. We will apply the Golay technique for measuring the impulse response and the amplitude and phase transfer functions of a linear magnetic tape recording channel. This channel suffers from nonlinear distortion caused by a magnetoresistive (MR) sensor. The measured characteristics will be compared with the same characteristics obtained with the de facto standard impulse response measurement technique using feedback shift register sequences. Based on a practical nonlinear model of our experimental tape recording channel, we will discuss the artefacts due to second and third order nonlinear distortion which can occur in the Golay impulse responses and transfer functions.

The outline of the next sections is as follows. In Section II, we will describe our measurement setup, and we will consider the signal-to-noise ratio (SNR) of the readback signal of our experimental tape recording channel. In Section III, we will focus on the de facto standard impulse response measurement technique using feedback shift register sequences. In Section IV, we will introduce a practical nonlinear model of our tape recording channel. In Section V, we will present the measured channel impulse response and amplitude and phase transfer functions obtained with the Golay technique, and we will analyze the artefacts due to second and third order nonlinear distortion which can occur in these characteristics.

## II. THE MEASUREMENT SETUP

Our measurement equipment uses a stationary-head instrumentation tape recorder, a programmable integrated read/write amplifier (OQ 8877 Philips IC), and a read/write head having a shielded MR sensor [8]. We use a write track width of about  $99 \mu\text{m}$ , and a read track width of about  $50.8 \mu\text{m}$ . Biasing of the MR element is achieved using a soft adjacent layer [10]. The read amplifier has a second order high-pass characteristic with a -3 dB cut-off frequency of about 6 kHz, and a flat amplitude characteristic in the passband. A binary excitation signal with a period of  $L$  symbols is written on tape (900 Oe chrome ferrite tape). Let  $\{a_i\} = \{a_0, a_1, \dots, a_i, \dots, a_{L-1}\}$ , where  $a_i \in \{\pm 1\}$ , denote a binary excitation sequence of length  $L$ . The write current has the form

$$w(t) = \sum_i a_{(i \bmod L)} p_T(t - iT), \quad (1)$$

where  $T$  denotes the symbol (or bit) duration, and  $p_T(t)$  denotes an ideal ‘full- $T$ ’ pulse, i.e.,

$$p_T(t) = \begin{cases} 1, & \text{for } -T/2 < t \leq T/2, \\ 0, & \text{else.} \end{cases} \quad (2)$$

We assume a noiseless linear time-invariant channel with dirac impulse response  $h(t)$ . The analog readback signal then is given by

$$r(t) = w(t) * h(t) = \sum_i a_{(i \bmod L)} h'(t - iT), \quad (3)$$

where  $*$  denotes linear convolution, and  $h'(t) = p_T(t) * h(t)$  is called the *dipulse response*. The readback signal is captured using a digital sampling oscilloscope under inclusion of an appropriate oversampling rate. In our experiments, we use the tape speed 16.9 cm/s and the excitation clock frequency  $1/T = 500$  kHz, which results in a minimum recorded wavelength of about 676 nm (2 bits per wavelength). Fig. 1 depicts the power spectrum of a readback signal after having recorded a sequence with white power spectrum. Further, the power spectra of tape running noise and tape stopped noise are shown. Apparently, the SNR is excellent, and the tape noise is hidden in the environmental noise floor. Fig. 1 indicates that the assumption of a noiseless channel is rather realistic.

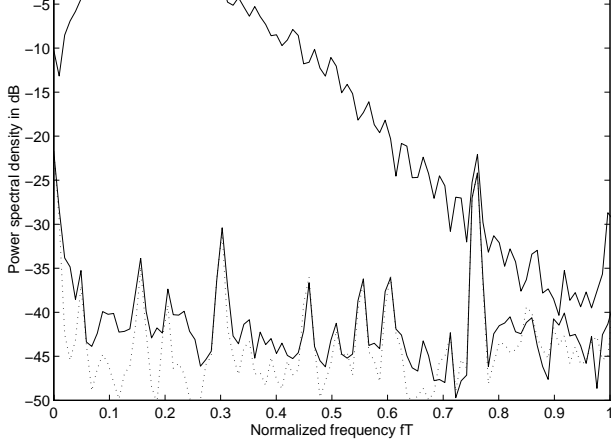


Fig. 1. Power spectrum of a readback signal after having recorded a sequence with white power spectrum, and power spectra of tape running noise (solid) and tape stopped noise (dotted).

### III. THE MLBS TECHNIQUE

We will start by considering the de facto standard impulse response measurement technique where the channel is probed with a feedback shift register sequence, or *Maximum Length Binary Sequence* (MLBS). This technique has been described in, for example, [9]. The MLBS key property we exploit for channel impulse response measurements is their well-behaved circular autocorrelation function. Cross correlating the captured waveform with the corresponding excitation MLBS results in the dipulse response, if the channel has no significant gain at DC. An MLBS is generated by a linear feedback shift register which can be defined by a primitive polynomial. The MLBS has period  $L = 2^m - 1$ , where  $m$  denotes the shift register length. A collection of MLBS properties can be found in, for example, [4]. We probe our experimental tape recording channel with the MLBS of 127 bit period defined by the polynomial  $z^7 + z^3 + 1$ , or alternatively by the recurrence  $a_i = a_{i-4}a_{i-7}$ . This MLBS was used by Palmer et al. [7] to characterize the read/write process for magnetic recording. The measured channel dipulse response obtained with this MLBS is depicted in Fig. 2. Apparently, there occur a few time delayed responses, or ‘echoes’, besides the main dipulse. As can be found in, for example, [3] or [7], these characteristic artefacts occurring in the MLBS dipulse response indicate the presence of nonlinear distortion in the readback signal.

### IV. A PRACTICAL NONLINEAR CHANNEL MODEL

Existing practical approaches to characterize nonlinear magnetic saturation recording channels, such as those described in, for example, [3] or [11], are based on Volterra input-output models. In addition to the linear dipulse response, these models include responses corresponding to multiplicative excitation terms of order greater or equal to two. We call these higher-order responses *Volterra kernels*. As indicated by Hermann [3] or Zeng and Moon [11], including a limited number of Volterra kernels is sufficient for a satisfying char-

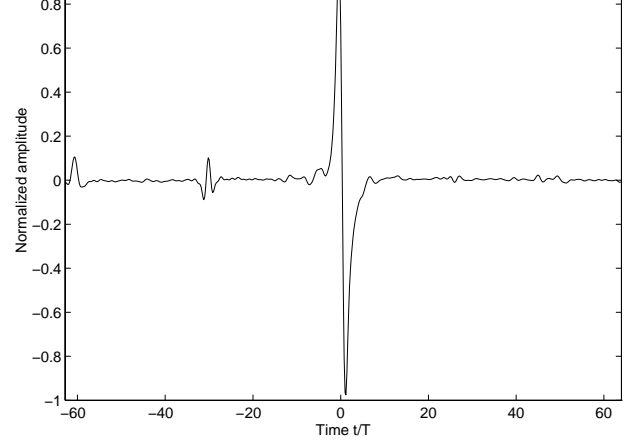


Fig. 2. Measured dipulse response obtained with MLBS defined by the polynomial  $z^7 + z^3 + 1$ .

acterization of nonlinear magnetic recording channels. As an example of such a nonlinear channel model, we consider a continuous-time Volterra model including four kernels. This model can be defined as follows. Let  $h^{(1)}(t) = h'(t)$  denote the linear channel dipulse response. Let further  $h_d^{(2)}(t)$  and  $h_{-1,1}^{(3)}(t)$  denote the Volterra kernels corresponding to the second order excitation term  $a_i a_{i-d}$ , and corresponding to the third order excitation term  $a_{i+1} a_i a_{i-1}$ , respectively. We include three second order Volterra kernels  $h_d^{(2)}(t)$  for  $d = 1, 2, 3$ , and we assume a noiseless time-invariant channel. The analog readback signal of this nonlinear channel is obtained as

$$r(t) = \sum_j a_j h^{(1)}(t - jT) + \sum_{d=1}^3 \sum_j (a_j a_{j-d}) h_d^{(2)}(t - jT) + \sum_j (a_{j+1} a_j a_{j-1}) h_{-1,1}^{(3)}(t - jT). \quad (4)$$

As we will see, this simple nonlinear channel model is sufficient for explaining the dominant echoes appearing in Fig. 2.

Hermann [3] derived the behavior of the MLBS technique in the presence of nonlinear distortion. He showed that the MLBS technique provides the sum of the linear dipulse response and the higher-order Volterra kernels, each kernel shifted by an amount varying from kernel to kernel and depending on the MLBS [3]. According to Hermann [3] and Palmer et al. [7], the echoes at positions  $-30T$  and  $-60T$  in Fig. 2 describe the Volterra kernels corresponding to the second order terms  $a_i a_{i-1}$  and  $a_i a_{i-2}$ , respectively. The main dipulse in Fig. 2 is corrupted by the Volterra kernel corresponding to the excitation term  $a_i a_{i-3}$  which appears at position  $-4T$ . According to Palmer et al. [7], the dominant echoes appearing in Fig. 2 are due to head asymmetry effects. The third order kernel  $h_{-1,1}^{(3)}(t)$  appearing at position  $25T$  in Fig. 2 has rather small amplitude compared to the amplitudes of the dominant second order Volterra kernels.

In this section, we will consider the impulse response measurement technique based on Golay complementary sequences [2]. A tutorial description of this technique can be found in, for example, [1].

### A. Preliminaries

Two Golay sequences  $\{a_i\}$  and  $\{b_i\}$  of length  $L$  have the property

$$\sum_j (a_j a_{n+j} + b_j b_{n+j}) = 2L \text{ if } n = 0, \text{ else } 0. \quad (5)$$

In other words, a pair of Golay complementary sequences has the property that the sum of both autocorrelation functions is an ideal discrete dirac impulse. This property holds for the linear and the circular autocorrelation functions, where in the circular case the indices are calculated modulo  $L$ . We will exploit this circular autocorrelation property for impulse response measurements. We will start by assuming a noiseless linear time-invariant channel characterized by the dipulse response  $h'(t)$ . We first probe the system with the Golay sequence  $\{a_i\}$ . The periodic output is sampled and correlated with  $\{a_i\}$  to produce the cross correlation sequence  $\{ca_n\}$ , given by

$$ca_n = \frac{1}{2L} \sum_j a_j r_{n+j} = \frac{1}{2L} \sum_j h'_j \sum_k a_{k-n} a_{k-j}, \quad (6)$$

where  $\{r_j\}$ ,  $r_j = r(jT)$ , denotes the sampled output sequence. The system is now probed again, this time using the sequence  $\{b_i\}$ . The output is sampled and correlated as before to produce another cross correlation sequence, denoted by  $\{cb_n\}$ . With the Golay property (5), the sum of the cross correlation sequences  $\{ca_n\}$  and  $\{cb_n\}$ , denoted by  $\{c_n\}$ , results in the dipulse response, i.e.,

$$c_n = ca_n + cb_n = h'_n. \quad (7)$$

In order to generate Golay sequences  $\{a_i\}_m$  and  $\{b_i\}_m$  of length  $L = 2^m$ , we use the following recursive algorithm. We start with the Golay pair  $\{a_i\}_1 = \{+1, +1\}$ ,  $\{b_i\}_1 = \{+1, -1\}$ , and we repeat recursively  $\{a_i\}_{m+1} = \{a_i\}_m | \{b_i\}_m$  and  $\{b_i\}_{m+1} = \{a_i\}_m | \{-b_i\}_m$ , where  $|$  denotes sequence concatenation.

### B. Experimental Results

Fig. 3 depicts the measured dipulse response of our experimental tape recording channel obtained with a pair of Golay complementary sequences of 128 bit length. Apparently, the Golay main dipulse in Fig. 3 is much less distorted than the MLBS main dipulse in Fig. 2. Compared to Fig. 2, the Golay dipulse response exhibits a higher level of noise-like distortion which is due to second order nonlinear distortion of the readback signal, as we will show below.

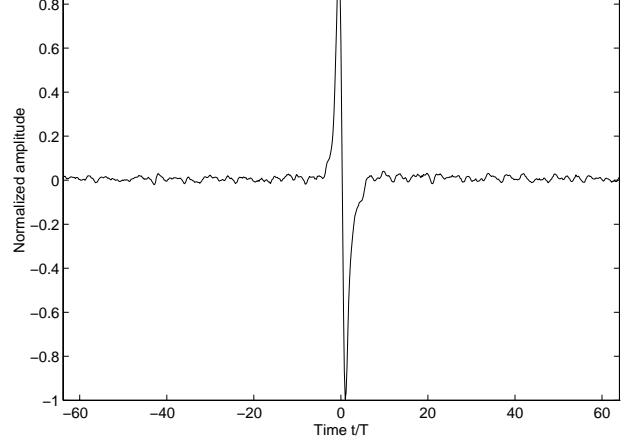


Fig. 3. Measured dipulse response obtained with Golay complementary sequences of 128 bit length.

Figs. 4 and 5 depict the measured channel amplitude and phase transfer functions obtained with the Golay technique and the MLBS technique. These transfer functions have been obtained from the dipulse responses in Fig. 3 and Fig. 2 by means of discrete Fourier transformation. Remarkably, the Golay technique results in a much more smooth amplitude transfer function than the MLBS technique. The dominant spikes occurring in the Golay amplitude transfer function in Fig. 4 are caused by second order nonlinear distortion of the readback signal, as we will show below. The phase transfer functions obtained with either of these techniques do not show remarkable differences. The notch appearing in the Golay phase transfer function in Fig. 5 is due to the arcus tangens uncertainty.

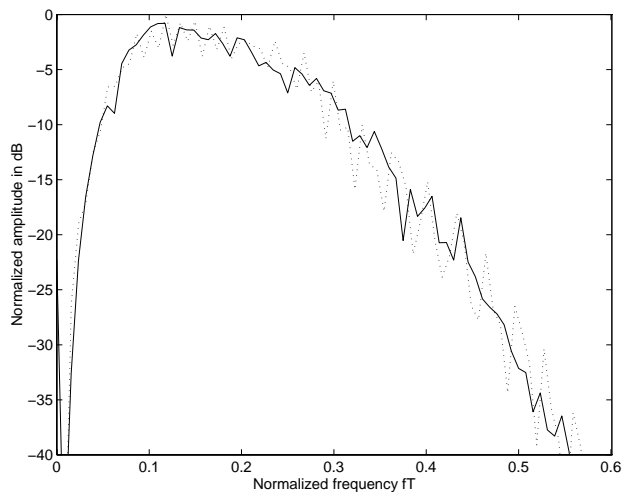


Fig. 4. Measured amplitude transfer functions obtained from the Golay dipulse response (solid) and the MLBS dipulse response (dotted).

### C. Waveform Synthesis

To assess the performances of the Golay and MLBS techniques, we will use the measured dipulse responses to syn-

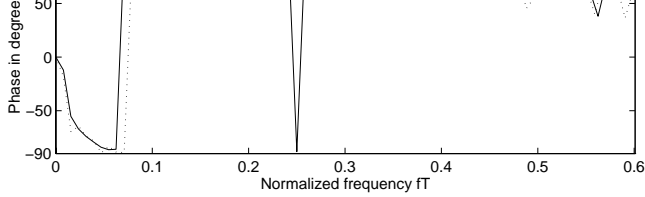


Fig. 5. Measured phase transfer functions obtained from the Golay dipulse response (solid) and the MLBS dipulse response (dotted).

thesize an arbitrary readback signal. Using a sampled estimate  $\{\hat{h}'_i\}$  of the channel dipulse response, we obtain by linear superposition an approximation  $\{\hat{r}_i\}$  of the captured readback signal, i.e.,  $\hat{r}_i = \sum_j a_j \hat{h}'_{i-j}$ . As a possible measure of the quality of our approximation, we define the signal-to-distortion ratio (SDR) by

$$10 \log_{10} \frac{\sum r_i^2}{\sum (\hat{r}_i - r_i)^2}.$$

We will start with the linear approximation of an arbitrary readback signal using the Golay dipulse response of Fig. 3. An example of a synthesized waveform is shown in Fig. 6. The resulting SDR is in the order of 16 dB. About the same SDR is obtained with the main MLBS dipulse of Fig. 2.

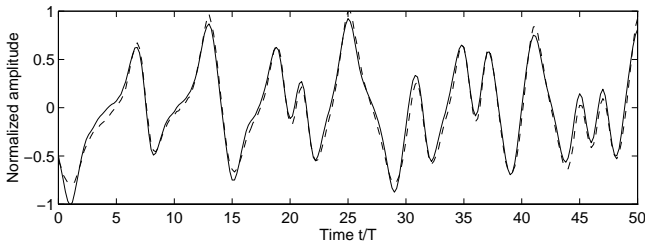


Fig. 6. Linear approximation (solid) of a captured readback signal (dashed) using the Golay dipulse response.

Using a simple nonlinear model of the readback signal, we achieve about 2 dB improvement in SDR versus the linear model. Our nonlinear model uses the Golay main dipulse of Fig. 3 as linear response and the Volterra kernels corresponding to the excitation terms  $a_i a_{i-1}$  and  $a_i a_{i-2}$ , extracted from Fig. 2. The improvement in SDR versus the linear signal model is rather marginal, but on the other hand it indicates causality between approximation error and amount of nonlinear distortion included in the model.

#### D. The Golay Technique in the Presence of Nonlinear Distortion

In this section, we will study the artefacts due to nonlinear distortion which occur in the Golay dipulse response and amplitude transfer function. We will assume a noiseless nonlinear time-invariant channel whose analog readback signal is given by (4). As derived elsewhere [13], the sampled dipulse response obtained with the Golay technique in the presence

$$c_n = h^{(1)}(nT) + \sum_{d=1}^3 h_d^{(2)}(nT) * g_d^{(2)}(n) + h_{-1,1}^{(3)}(nT) * g_{-1,1}^{(3)}(n), \quad (8)$$

where

$$g_d^{(2)}(n) = \frac{1}{2L} \sum_k (a_k a_{k+n} a_{k+n-d} + b_k b_{k+n} b_{k+n-d}),$$

and

$$g_{-1,1}^{(3)}(n) = -\frac{1}{2} \text{ if } n = \pm 2, \text{ else } 0,$$

and  $*$  denotes circular convolution, i.e.,

$$a_n * b_n = \sum_j a_j b_{n-j},$$

where the indices are calculated modulo  $L$ . Below, we will briefly discuss expression (8) for the sequence length  $L = 128$ .

We will start by considering the effect of second order nonlinear distortion on the Golay dipulse response. As an example, the Golay correlation term  $g_1^{(2)}(n)$  is shown in Fig. 7. The Golay correlation terms  $g_d^{(2)}(n)$  for  $d = 2, 3$  result

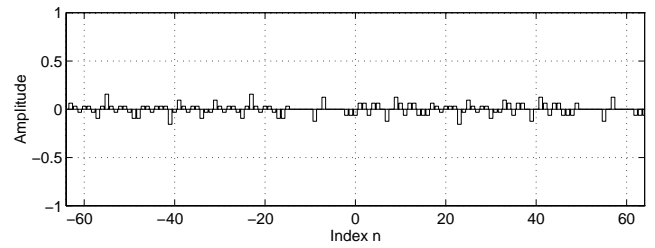


Fig. 7. Golay correlation term  $g_1^{(2)}(n)$ .

in basically similar characteristics as for  $d = 1$ . We conclude that the Golay technique spreads the relevant observed second order Volterra kernels throughout the time domain. This theoretically derived behavior of the Golay dipulse response in the presence of second order nonlinear distortion is in good agreement with the result of Fig. 3 obtained in a real measurement. Similar artefacts in the Golay dipulse response caused by second order nonlinear distortion were obtained by Norcross and Vanderkooy [5] in computer simulations. The superposition of second order nonlinear distortion terms  $h_d^{(2)}(nT) * g_d^{(2)}(n)$  in the Golay dipulse response may be constructive or destructive, depending on the particular characteristics of occurring second order Volterra kernels  $h_d^{(2)}(t)$ . Therefore, the Golay dipulse response does not allow to quantify the amount of second order nonlinear distortion present on the channel.

In the Golay amplitude transfer function, second order nonlinear distortion may cause remarkable artefacts at certain characteristic frequencies. As follows from (8), this property is found by analyzing the amplitude spectra of the

plays the amplitude spectrum of the superposed Golay correlation term  $\sum_{d=1}^3 g_d^{(2)}(n)$ . Those frequencies for which the amplitude spectrum in Fig. 8 exceeds the 0 dB level are in perfect alignment with the frequencies at which the measured Golay amplitude spectrum in Fig. 4 exhibits remarkable artefacts.

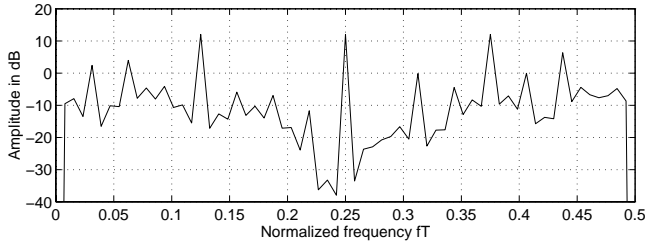


Fig. 8. Amplitude spectrum of the superposed Golay correlation term  $\sum_{d=1}^3 g_d^{(2)}(n)$ . The 0 dB level corresponds to the amplitude spectrum of a discrete dirac impulse of unity amplitude.

Third order nonlinear distortion has a different effect on the Golay dipulse response as second order nonlinear distortion. As follows from (8), a distortion term

$$-\frac{h_{-1,1}^{(3)}((n+2)T) + h_{-1,1}^{(3)}((n-2)T)}{2}$$

caused by third order nonlinear distortion is immediately corrupting the Golay main dipulse. Therefore, the Golay dipulse response does not allow to quantify the amount of third order nonlinear distortion present on the channel. In the Golay amplitude transfer function, third order nonlinear distortion may be present over a wide frequency range. This property follows from the amplitude spectrum of the Golay correlation term  $g_{-1,1}^{(3)}(n)$ , given by  $|\cos(4\pi fT)|$ . As in our experiments occurring third order nonlinear distortion effects are rather weak, we can not for certain demonstrate the artefacts in the Golay dipulse response caused by these effects. We have confined our analysis of third order nonlinear distortion effects to the Volterra kernel corresponding to the excitation term  $a_{i+1}a_i a_{i-1}$ . Other third order Volterra kernels corresponding to excitation terms  $a_{i-d_1}a_i a_{i-d_2}$  for small integers  $(d_1, d_2)$  different from  $(-1, 1)$  turned out to result in similar artefacts as for  $(d_1, d_2) = (-1, 1)$ .

We have exploited the circular autocorrelation property of Golay complementary sequences for impulse response measurements. In certain applications, such as those described in, for example, [1], [5], or [12], it is more appropriate to exploit the linear autocorrelation property of Golay complementary sequences for impulse response measurements. If linear correlations are performed, the artefacts due to second and third order nonlinear distortion which occur in the Golay dipulse response and amplitude transfer function have similar characteristics as discussed above.

## VI. CONCLUSIONS

We applied Golay complementary sequences for measuring the impulse response and the amplitude and phase transfer

function caused by an MR sensor. The measured characteristics, in particular the amplitude transfer function, showed better performance than the same characteristics obtained with the de facto standard impulse response measurement technique using feedback shift register sequences. Based on a practical nonlinear model of our experimental tape recording channel, we discussed the artefacts due to second and third order nonlinear distortion which can occur in the Golay impulse responses and transfer functions. We showed that these characteristics do not allow to quantify the amount of nonlinear distortion present on the channel. In the Golay dipulse response, second order kernels, such as caused by, for example, asymmetry effects of MR heads [7], appear spread throughout the time domain. We further showed that third order nonlinear kernels, such as caused by, for example, saturation introduced by an MR sensor [7], or transition shifts due to demagnetizing fields during the write operation [6], result in a corruption of the Golay main dipulse.

## ACKNOWLEDGMENTS

The experimental part of this research study has been carried out at the Philips Research Laboratories in Eindhoven, The Netherlands. The author would like to thank K.A.S. Immink, S.B. Luitjens, and all other members of the Magnetic Recording group for helpful discussions and comments.

## REFERENCES

- [1] S. Foster, "Impulse Response Measurement Using Golay Codes," *Trans. ICASSP '86*, pp. 929-932, 1986.
- [2] M.J.E. Golay, "Complementary Series," *IRE Trans. Inform. Theory*, vol. 7, pp. 82-87, April 1961.
- [3] R. Hermann, "Volterra Modeling of Digital Magnetic Saturation Recording Channels," *IEEE Trans. Magn.*, vol. MAG-26, no. 5, pp. 2125-2127, September 1990.
- [4] F.J. MacWilliams, and N.J.A. Sloane, "Pseudo-Random Sequences and Arrays," *Proceedings of the IEEE*, vol. 64, no. 12, pp. 1715-1730, December 1976.
- [5] S. Norcross, and J. Vanderkooy, "A Survey of the Effects of Nonlinearity on Various Types of Transfer-Function Measurements," *Preprint 4137 (H-2) of the 99th AES Convention New York*, Audio Eng. Soc., October 1995.
- [6] D. Palmer, P. Ziperovich, R. Wood, and T.D. Howell, "Identification of Nonlinear Write Effects Using Pseudorandom Sequences," *IEEE Trans. Magn.*, vol. MAG-23, no. 5, pp. 2377-2379, September 1987.
- [7] D. Palmer, J. Hong, D. Stanek, and R. Wood, "Characterization of the Read/Write Process for Magnetic Recording," *IEEE Trans. Magn.*, vol. MAG-31, no. 2, pp. 1071-1076, March 1995.
- [8] R.I. Potter, "Digital Magnetic Recording Theory," *IEEE Trans. Magn.*, vol. MAG-10, pp. 502-508, 1974.
- [9] M.R. Schroeder, "Integrated-Impulse Method Measuring Sound Decay without Using Impulses," *J. Acoust. Soc. Am.*, vol. 66, pp. 497-500, August 1979.
- [10] C. Tsang, "Magnetics of Small Magnetoresistive Sensors," *J. Appl. Phys.*, 55 (6), pp. 2226-2231, March 1984.
- [11] W. Zeng, and J. Moon, "A Practical Nonlinear Model for Magnetic Recording Channels," *IEEE Trans. Magn.*, vol. MAG-30, no. 6, pp. 4233-4235, November 1994.
- [12] B. Zhou, D.M. Green, and J.C. Middlebrooks, "Characterization of External Ear Impulse Responses Using Golay Codes," *J. Acoust. Soc. Am.*, 92 (2), Pt.1, pp. 1169-1171, August 1992.
- [13] V. Braun, "manuscript to appear in the author's doctoral thesis," August 1996.